DOI: 10.37190/abb/235938

Evaluation of local quadriceps action response patterns during cycling using a multimodal NIRS and thermal imaging protocol: a pilot study

Adam Suchański[1], Aleksandra Mrowiec[2], Zuzanna Kowalczyk[2], Armand Cholewka[3], Manuel Sillero-Quintana[4], Agata Stanek[5,6], Teresa Kasprzyk-Kucewicz[3,*]

[1]Centre for Physical Education and Sport, University of Silesia, Katowice, Poland

[2]Faculty of Science and Technology, University of Silesia, Chorzów, Poland

[3]Institute of Biomedical Engineering, Faculty of Science and Technology, University of Silesia, Chorzów, Poland

[4]Faculty of Physical Activity and Sport Sciences (INEF), Universidad Politécnica de Madrid, Spain

[5]Department of Internal Medicine and Metabolic Diseases, Faculty of Health Sciences in Katowice, Medical University of Silesia, Poland.

[6]Upper-Silesian Medical Centre of the Medical University of Silesia in Katowice, Katowice, Poland.

[*]Corresponding author: Teresa Kasprzyk-Kucewicz, Institute of Biomedical Engineering, Faculty of Science and Technology, University of Silesia, Chorzów, Poland, e-mail address: teresa.kasprzyk-kucewicz@us.edu.pl

Submitted: 20th April 2026

Accepted: 2nd September 2026

Abstract:

Purpose: This study aimed to develop and evaluate a comprehensive physiological testing protocol for cyclists that integrates thermal imaging and near-infrared spectroscopy during standardized incremental exercise. **Methods:** Eight trained male cyclists performed a standardized incremental cycling test under controlled conditions. After a 10-minute warm-up (1.0 $W \cdot kg^{-1}$), workload increased by 0.5 $W \cdot kg^{-1}$ every 3 minutes until voluntary exhaustion, followed by a 10-minute cool-down. Muscle oxygen saturation (SmO_2) of the rectus femoris was continuously recorded bilaterally using wearable near-infrared spectroscopy (Moxy Monitor), and thermal imaging of selected quadriceps muscles was conducted with a FLIR T1020 camera. Heart rate was monitored continuously. Measurements were performed after a 25-minute acclimatization period under standardized environmental conditions. **Results:** No statistically significant differences in normalized skin temperature (T_{sk}) or normalized SmO_2 were observed across exercise phases after Bonferroni correction ($p = 0.012$). A significant positive correlation was found between exercise-induced changes in normalized T_{sk} and SmO_2 (ΔEX: Spearman's $r = 0.89$, $p << 0.017$). No significant correlation was observed during the warm-up (ΔWU: $r = 0.02$) or recovery (ΔCD: $r = 0.14$) phases. Due to the small sample size ($n = 8$), correlations were interpreted descriptively as indicative of a physiological connection rather than causal relationships. **Conclusions:** Increasing exercise intensity was associated with concurrent alterations in muscle oxygenation and T_{sk}, reflecting integrated hemodynamic and metabolic responses. The combined IRT–NIRS protocol demonstrated methodological feasibility and may provide a valid framework for multidimensional assessment of muscular responses, warranting further validation in larger cohorts.

Keywords: Metabolism, Thermography, Exercise, Near-Infrared Spectroscopy, Body temperature regulation

1. Introduction

Exercise physiology in endurance sports provides a basis for effectively planning and improving training by explaining how the body can sustain prolonged physical activity while maintaining internal homeostasis [15]. In disciplines such as cycling, physical effort is inherently complex, involving the interaction of both aerobic and anaerobic metabolic pathways. Aerobic metabolism predominates during prolonged submaximal exercise, whereas anaerobic metabolism plays a crucial role during short, high-intensity efforts such as sprints or uphill climbs [10],[19]. The circulatory and respiratory systems are essential for sustaining

endurance performance, as they ensure the delivery of oxygen to working muscles and facilitate the removal of metabolic by-products [23],[30].

Training intensity is assessed and regulated based on measurable physiological parameters, including heart rate (HR), oxygen uptake (VO_2), and maximal oxygen uptake (VO_2 max). These parameters are considered primary indicators of aerobic capacity [4],[15],[30]. An additional key component of training optimization is the determination of metabolic thresholds, particularly the lactate and anaerobic thresholds, which define exercise intensity domains that promote endurance adaptations while limiting excessive metabolic disturbance [6],[15],[19],[38].

Practical endurance training requires the appropriate selection of training methods and their systematic distribution over time. Periodization of the training year, based on structured training cycles, enables the gradual development of physical fitness and the attainment of peak performance during competition periods, while accounting for recovery processes and supercompensation mechanisms [5],[13],[27],[32]. Consequently, understanding the relationship between training load and physiological adaptation is fundamental to effectively optimizing endurance performance.

The optimal functioning of the human body depends on effective temperature regulation, as maintaining a stable body temperature is essential for the proper functioning of the nervous, cardiovascular, and skeletal systems [14],[16]. The body maintains its core temperature within a tight range of about 36.5 to 37.5 ℃, and moving outside this range can disrupt its function and lead to serious health issues [17],[39]. The hypothalamus governs the thermoregulatory system, which maintains thermal stability. This system gathers information from both peripheral and central thermoreceptors and adjusts the body's mechanisms for producing and losing heat [2],[14].

Metabolic processes are responsible for most increases in internal body temperature. Under resting conditions, heat loss to the surroundings offsets the heat produced; however, during physical activity, the body's metabolic rate increases rapidly, resulting in a significant rise in heat production in the working muscles [17]. As a result, skeletal muscles become the primary source of heat, and their temperature rises above resting levels [16],[39].

These thermoregulatory processes are not straightforward, as thermoregulatory reflexes often occur alongside other non-thermoregulatory mechanisms, such as baroreceptor-mediated blood pressure regulation. This interaction might cause temporary issues with blood vessel regulation, especially during the early stages of physical activity [20],[22]. As a result, an increase in core

body temperature increases blood flow to the skin and triggers sweating, making evaporative cooling the primary way the body loses heat [2],[14].

The Pennes bioheat equation describes heat transfer within living tissues by combining heat conduction with metabolic heat production and blood perfusion [24],[28]. The following formula gives the currently accepted version of Pennes' equation:

$$\boldsymbol{c(T)\frac{\partial T(x,t)}{\partial t} = \nabla[\beta(T)\nabla T(x,t)] + Q_{perf}(x,t) + Q_{met}} \quad (1)$$

where:

$\boldsymbol{\beta}$ – tissue conductivity coefficient [W/m·K],

$\boldsymbol{c}$ – specific heat of tissue per unit volume (product of specific heat and mass density),

$\boldsymbol{Q_{perf}}$ – a component related to blood perfusion,

$\boldsymbol{Q_{met}}$ – a component related to metabolism,

The relationship gives the component describing blood perfusion, $\boldsymbol{Q_{perf}}$:

$$\boldsymbol{Q_{perf} = G_B c_B [T_B - T(x,t)]} \quad (2)$$

where:

$\boldsymbol{G_B}$ – perfusion coefficient,

$\boldsymbol{c_B}$ – specific heat capacity of blood,

$\boldsymbol{T_B}$ – blood temperature,

$\boldsymbol{T(x,t)}$ - temperature field of the tissue under consideration.

The Q_{met} value varies with body conditions, ranging from 245 to 24500 W/m^3 [24],[28]. The metabolic term reflects local heat generation, whereas the perfusion term accounts for energy exchange between blood and tissue, dependent on blood flow magnitude and temperature gradients [18]. In the present study, the Pennes bioheat equation is presented solely as a conceptual framework for understanding the physiological mechanisms underlying heat transfer during exercise, rather than as a model directly validated by the experimental data.

Near-infrared spectroscopy (NIRS) is a non-invasive technique used to assess local changes in skeletal muscle oxygenation at rest, during exercise, and throughout recovery. The method is based on the differential absorption properties of hemoglobin and myoglobin in the near-infrared spectrum (approximately 650–900 nm), enabling the evaluation of the balance between oxygen delivery and utilization in working muscles [8],[29].

NIRS allows continuous monitoring of changes in oxygenated (O_2Hb) and deoxygenated (HHb) hemoglobin and myoglobin, as well as the derived parameter, muscle oxygen saturation (SmO_2). SmO_2 is currently the most commonly used variable in exercise studies, as it integrates information on oxygen supply and extraction and is relatively insensitive to changes in tissue blood volume [11]. At the onset of exercise, SmO_2 typically decreases rapidly due to an abrupt increase in metabolic demand and oxygen extraction. During steady-state exercise, the partial pressure of oxygen (pO_2) may stabilize when the rate of oxygen delivery matches the rate of oxygen utilization. In contrast, during incremental exercise, pO_2 progressively declines to minimal values near exhaustion, indicating limitations in muscle oxidative capacity [8].

The findings indicate that NIRS has the potential to function as an effective instrument for determining exercise thresholds in both laboratory and field settings.

During post-exercise recovery, SmO_2 typically increases rapidly, often exceeding resting values, a phenomenon known as post-exercise hyperemia. The rate of muscle reoxygenation serves as an indicator of microcirculatory efficiency and training adaptation, providing valuable insight into an athlete's training status and recovery capacity [29],[34].

The present study aims to propose a comprehensive physiological testing protocol for cyclists that integrates thermal imaging, muscle oxygen saturation assessment using near-infrared spectroscopy (Moxy sensor), and body composition analysis under standardized incremental exercise conditions. This integrated approach enables a multidimensional characterization of the physiological responses to increasing exercise intensity and may serve as a practical tool for performance diagnostics and training optimization.

2. Materials and Methods

2.1. Participants

The study was conducted on a group of eight male cyclists at the Laboratory of Sports Medicine, Faculty of Science and Technology, University of Silesia in Chorzów, Poland. All participants had training experience exceeding six years. During the year preceding the study, the volunteers engaged in regular sports training, with weekly volumes ranging from 10 to 14 hours. Basic anthropometric and somatic characteristics, including body mass, height, body mass index (BMI), and body fat percentage, were assessed before the experiment and presented in Table 1. All volunteers had their right leg as their dominant leg.

Table 1. Characteristics of the study group.

	Age [years]	**Height [cm]**	**Body mass [kg]**	**Body fat [%]**	**Muscle mass [kg]**	**TBW [%]**	**BMI [kg/m²]**	**HR_{pre} [bpm]**	**HR_{max} [bpm]**

Mean	34.6	178.0	75.9	10.6	64.5	60.2	24.0	74.0	180.3
SD	6.1	7.3	4.9	3.0	4.4	2.3	1.4	8.3	8.0

TBW – total body water expressed as a percentage of total body mass, BMI – body mass index, HR_{pre} - pre-exercise heart rate, HR_{max} – maximum heart rate during training.

Inclusion criteria included the absence of cardiovascular, metabolic, or neuromuscular disorders, no recent musculoskeletal injuries, and refraining from intensive training for at least 48 hours before the measurements. Exclusion criteria included acute illness, the use of analgesic or antipyretic medications, alcohol consumption within 48 hours before testing, and participation in cryotherapy treatments or sauna sessions during the same period. These criteria were adopted in accordance with the guidelines for medical thermal imaging measurements established by the European Thermology societies [1],[25].

The study was conducted in accordance with the ethical standards of the Declaration of Helsinki and was approved by the Ethics Committee of the Medical University of Silesia (protocol code BNW/NWN/0052/KB1/78/25, approved on 8 July 2025). All participants provided written informed consent before participation.

2.2.Research protocol

The research protocol included body composition analysis, placement of a near-infrared spectroscopy sensor on the quadriceps muscles, and continuous thermal imaging. Subsequently, a graded exercise test was performed on a bicycle ergometer.

The test began with a 10-minute warm-up at a low workload corresponding to 1.0 $W \cdot kg^{-1}$. This was followed by a progressive exercise test in which the workload was increased by approximately 0.5 $W \cdot kg^{-1}$ every 3 minutes [3],[31]. The test was terminated upon voluntary exhaustion or when the supervising staff deemed termination necessary. After completion of the test, participants performed a 10-minute cool-down phase at a workload below 1.0 $W \cdot kg^{-1}$. The total duration of the exercise protocol (excluding the cool-down phase) was 29.25 ± 2.5 minutes, depending on individual performance capacity, and ranged from 28 to 35 minutes. The graded exercise test was conducted on a bicycle ergometer Tacx Neo 2T Smart (TACX, Netherlands). Participants maintained a constant cadence of 80-90 rpm throughout the test. Ambient laboratory conditions were controlled and maintained at 21.3 ± 0.9 °C and 52 ± 2 % relative humidity.

2.3. NIRS and heart rate measurements

A near-infrared spectroscopy sensor (Moxy Monitor, Fortiori Design LLC, USA) was placed over the central portion of the rectus femoris muscle belly, approximately at two-thirds of the muscle length measured from the proximal attachment, to expose the largest possible surface area for thermal imaging. Muscle oxygen saturation (SmO_2) was recorded continuously throughout the test from both left and right legs. The acquisition and analysis of SmO_2 were performed using PerfPro Studio 2022 and PerfPro Analyzer 2022 software, respectively.

Heart rate was continuously recorded using a Garmin HRM-Dual chest strap connected via ANT+ technology to the Tacx Desktop App (software version 4.41). Each participant performed the test on their own bicycle, which was mounted on a stationary trainer equipped with a freehub body compatible with Shimano/SRAM systems, using the cassette commonly installed on the cyclist's bike. To standardize the experimental protocol and ensure high measurement repeatability, all participants used the same gear configuration: the smallest rear sprocket and the largest front chainring. Additionally, all cyclists used round chainrings and 11-speed rear cassettes.

The Moxy sensor was placed on the belly of the rectus femoris, one of the primary muscles involved in power production during cycling. Previous electromyographic studies have demonstrated substantial activation of the rectus femoris throughout the pedaling cycle, reflecting its dual role in knee extension and hip flexion, which makes it a suitable site for monitoring local muscle oxygenation during cycling exercise [9].

2.4.Thermal imaging measurements

Thermal imaging tests were conducted using a FLIR Systems T1020 camera with a detector resolution of 1024 × 768 pixels and a thermal sensitivity/NETD of 20 mK. The camera was mounted on a tripod at a distance of 1.2 ± 0.1 m from the participant, positioned perpendicular to the imaged surface, i.e., the frontal plane of the thigh during knee extension. Thermal images were recorded continuously throughout the exercise test as a radiometric video, preserving full temperature information for each pixel in every frame and enabling detailed post-processing and temporal analysis of skin surface temperature changes. The applied protocol enabled continuous data collection without requiring the cyclist to interrupt the exercise.

Before the measurements, participants underwent a 25-minute acclimatization period to the testing laboratory's thermal conditions, during which they remained seated at rest. At the same

time, the body regions to be imaged were exposed. Skin emissivity was set to 0.98. The examined skin areas were clean, dry, and free of cosmetics [1],[25].

Thermal image sequences were analyzed using FLIR Thermal Studio PRO software. Regions of interest (ROI) were defined for selected lower-limb muscle groups, including the rectus femoris muscle (RECT_FEM), the vastus lateralis muscle (VAS_LAT), and the vastus medialis muscle (VAS_MED). The same experienced investigator delineated all ROIs. The locations of individual ROIs for both legs are shown in Figure 1 for a representative athlete.

The location of the Moxy sensor required partial coverage of the examined muscle group. Therefore, the analyzed regions of interest (ROI) were correspondingly limited. The position of the Moxy sensor for a representative participant's legs during knee extension is shown in Figure 1.

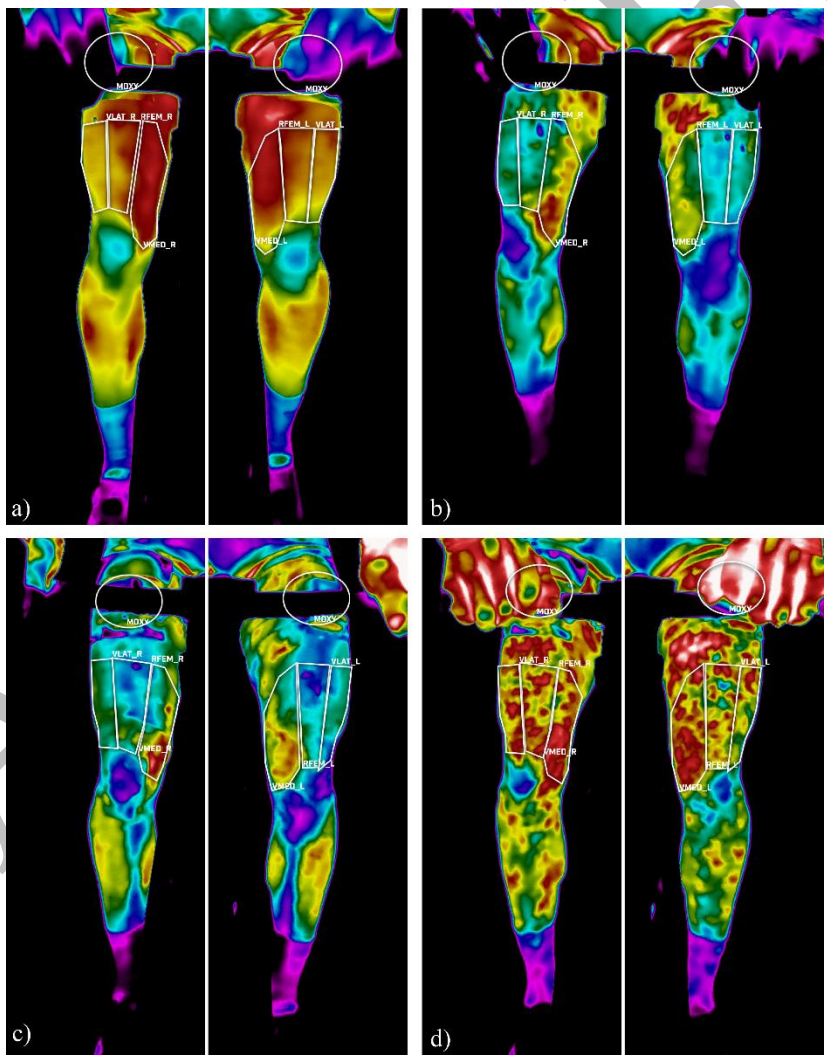

Figure 1. Thermal images of a representative athlete's left and right legs are shown: (a) before exercise, (b) after 10 minutes, (c) during the final minutes of exercise, and (d) after the cool-down phase with sensor Moxy placement.

2.5.Statistical analysis

Statistical analysis was performed using STATISTICA ver. 13. Data normality was assessed using the Shapiro–Wilk test, while homogeneity of variances was verified with Levene's test. All analyzed variables, i.e., SmO_{2_rel} and T_{sk_rel}, did not meet the assumption of normality; therefore, nonparametric statistical methods were applied. Changes in physiological and thermal parameters across exercise stages were analyzed using the Friedman test or Spearman's rank correlation. The level of statistical significance was set at $p < 0.05$.

When the Friedman test indicated a significant overall effect, post hoc pairwise comparisons were performed using the Wilcoxon signed-rank test with a Bonferroni correction (adjusted significance level determined by the number of pairwise comparisons). Effect sizes for the Friedman test were expressed as Kendall's coefficient of concordance (*W*). For the primary correlation analysis, 95% confidence intervals were additionally reported. Data are presented as median and interquartile range (IQR).

3. Results

Representative thermal images obtained for selected phases of the exercise protocol are presented in Figure 1.

Due to inter-individual differences in resting T_{sk} among athletes within the groups, T_{sk} normalization was applied to obtain relative skin temperature values (T_{sk_rel}) and to standardize the results, allowing trends in skin temperature changes to be examined across age categories. The normalization was performed according to the following equation

$$T_{sk\_rel} = T_{sk\_i} - T_{sk\_pre} \quad (3)$$

where $T_{sk\ i}$ represents the T_{sk} at a given imaging time point and T_{pre} denotes the pre-exercise T_{sk}.

The median T_{sk} values together with the interquartile range (IQR) for the analyzed phases are presented in Table 2, whereas the normalized values (T_{sk_rel}) illustrating the relative changes in skin temperature are shown in Figure 2.

Changes in the normalized median T_{sk_rel} for selected key training phases across individual muscle groups are shown in Figure 2. The selected phases correspond to moments in training when changes occur in both muscle perfusion and metabolism, and when physiological

reactions responsible for the athlete's performance occur. The T_{sk_rel} selected were before training, after warm-up, after exercise, and after the cool-down phase.

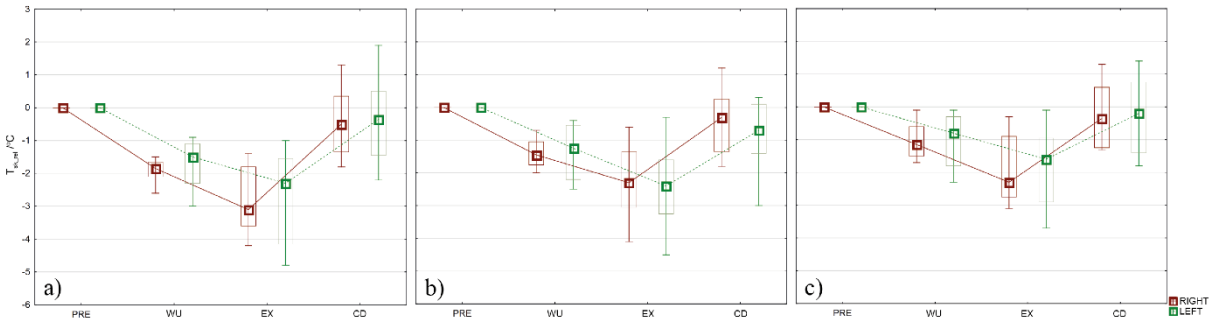

Figure 2. Temporal changes in Tsk_rel across exercise phases: PRE (pre-exercise), WU (post–warm-up), EX (post-exercise), and CD (post–cool-down) for a) the rectus femoris, b) the vastus lateralis, and c) the vastus medialis muscles for right (red) and left (green) leg. Data are presented as median values, with boxes representing the interquartile range (25th–75th percentile), and whiskers indicate the non-outlier range.

Table 2. Skin temperature (T_{sk}) values presented as median (Q1–Q3) for the analyzed exercise phases.

Median skin temperature /°C				
	PRE	WU	EX	CD
RECT_FM L	31.60 (30.93-32.00)	29.75 (29.28-30.53)	29.20 (27.68-30.33)	31.40 (30.70-31.80)
RECT_FM R	31.65 (31.00-32.45)	29.55 (29.28-30.80)	29.35 (28.08-29.50)	31.15 (30.98-31.45)
VAS_LAT L	31.15 (30.88-31.53)	29.85 (29.00-30.75)	28.85 (28.28-29.60)	30.60 (30.78-31.30)
VAS_LAT R	31.50 (30.60-31.93)	29.85 (29.23-31.03)	29.20 (29.23-31.03)	31.15 (28.80-30.88)
VAS_MED L	31.85 (31.60-32.70)	31.10 (30.50-31.88)	30.45 (29.33-31.55)	31.95 (31.58-32.35)
VAS_MED R	31.85 (31.18-32.60)	30.80 (30.45-31.93)	30.50 (29.20-30.78)	31.80 (31.58-32.23)

where: PRE - pre-exercise, WU - post–warm-up, EX - post-exercise, CD - post–cool-down; L – left side, R – right side.

Changes in T_{sk_rel} across exercise phases were analyzed separately for the right and left limbs using the Friedman ANOVA. The Friedman test demonstrated significant differences in normalized Tsk_rel across exercise phases for all analyzed muscles and both limbs ($\chi^2(3) = 16.97 – 20.85$, all $p < 0.001$; Kendall's $W = 0.71 – 0.87$), indicating a strong overall effect of exercise phase. Post hoc pairwise comparisons were subsequently performed using the Wilcoxon signed-rank test with Bonferroni correction (adjusted significance level: $p < 0.008$). However, none of the pairwise comparisons remained statistically significant after correction. The lowest p-value obtained in the post hoc analysis was 0.012, which did not reach the adjusted significance threshold.

Muscle oxygen saturation (SmO_2) was analyzed to characterize local muscle oxygenation dynamics across the exercise protocol. Due to substantial inter-individual variability in absolute SmO_2 values, the data were normalized relative to the pre-exercise baseline to obtain relative

muscle oxygen saturation values (SmO_{2_rel}), enabling comparison of relative changes between participants [12].

Normalization was performed according to the following equation:

$$SmO_{2\_rel} = SmO_{2_i} - SmO_{2_{pre}} \quad (4)$$

where $SmO_{2\ i}$ - represents the value recorded at a given time point, and $SmO_{2\ pre}$ - denotes the values obtained before the training protocol.

SmO_2 responses were evaluated at four key time points, similarly to T_{sk}: before training, after warm-up, after exercise, and after the cool-down phase. This approach allows the assessment of relative changes in muscle oxygenation independent of baseline differences, reflecting the balance between oxygen delivery and utilization during successive exercise phases. The median SmO_2 values and interquartile ranges (IQRs) for the analyzed phases are presented in Table 3. Results for the relative SmO_2 level are shown in Figure 3.

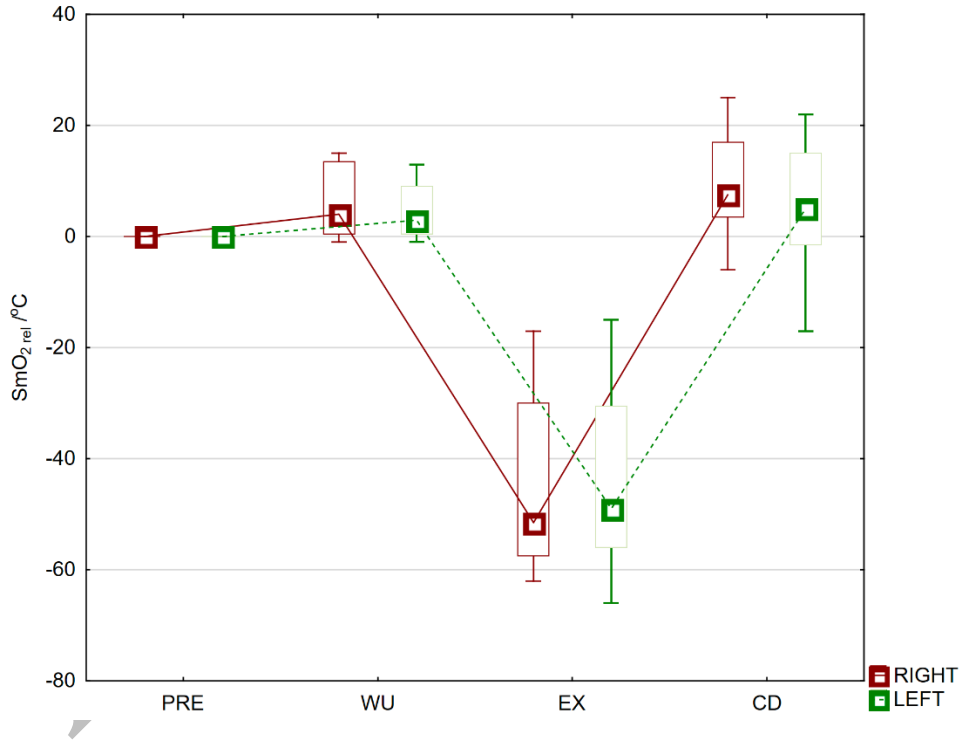

Figure 3. Median changes in relative muscle oxygen saturation (SmO_2_rel) across successive exercise phases: PRE (pre-exercise), WU (post–warm-up), EX (post-exercise), and CD (post–cool-down) for right (red) and left (green) leg. Data are presented as median values, with boxes representing the interquartile range (25th–75th percentile), and whiskers indicate the non-outlier range.

Table 3. Muscle oxygen saturation (SmO_2) values presented as median (Q1-Q3) for the analyzed exercise phases.

Muscle oxygen saturation /%				
	PRE	WU	EX	CD
RECT_FM L	73.00 (64.75-82.00)	82.50 (68.25-87.25)	28.50 (13.75-42.50)	83.50 (76.50-87.00)
RECT_FM R	68.50 (59.25-82.75)	78.00 (69.75-86.50)	22.50 (15.00-33.75)	84.50 (76.00-85.50)

where: PRE - pre-exercise, WU - post–warm-up, EX - post-exercise, CD - post–cool-down; L – left side, R – right side.

Changes in SmO_{2_rel} across exercise phases were analyzed separately for the right and left limbs using the Friedman test. The Friedman test revealed significant overall differences in normalized SmO_{2_rel} across exercise phases for both limbs ($\chi^2(3) = 17.09 – 17.65$, all $p < 0.001$), with Kendall's coefficients of concordance (W) ranging from 0.71 to 0.74, indicating a strong overall effect of exercise phase. Post hoc pairwise comparisons were subsequently performed using the Wilcoxon signed-rank test with Bonferroni correction (adjusted significance threshold: $p < 0.008$). However, none of the pairwise comparisons reached the adjusted significance threshold; the lowest observed *p*-value was 0.012.

The relationship between changes in T_{sk_rel} and alterations in normalized SmO_{2_rel} for the rectus femoris muscle was assessed separately for the warm-up, exercise, and cool-down phases using Spearman's rank correlation. Change scores were calculated as follows: ΔWU was defined as the difference between post–warm-up and pre-exercise values (WU-PRE), reflecting the acute preparatory response to increasing metabolic demand; ΔEX as the difference between post-exercise and post–warm-up values (EX-WU), representing the primary exercise-induced response; and ΔCD as the difference between post–cool-down and post-exercise values (CD-EX), corresponding to the early recovery phase. A Bonferroni-adjusted significance level of $p < 0.017$ was applied. Results are shown in Figure 4.

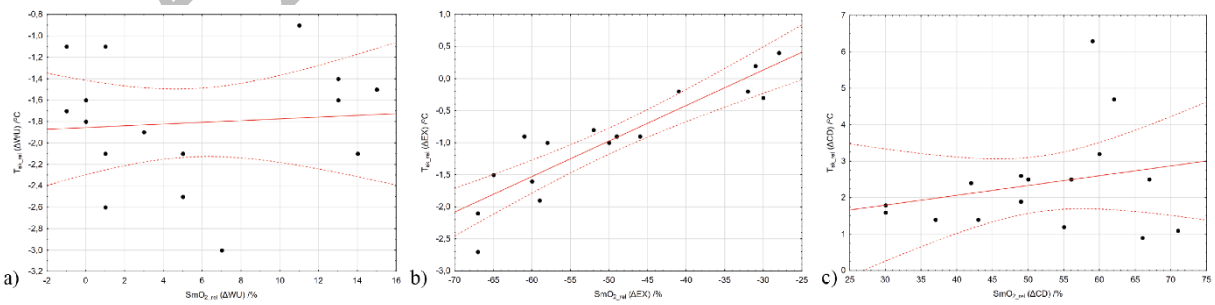

Figure 4. Scatter plots illustrating the relation between changes in Tsk_rel and alterations in relative muscle oxygen saturation (SmO_2_rel) assessed using Spearman's rank correlation: a) ΔWU (post–warm-up − pre-exercise), b) ΔEX (post-exercise − post–warm-up), and c) ΔCD (post–cool-down − post-exercise).

A statistically significant correlation was observed for ΔEX, defined as the difference between post-exercise and post-warm-up values (EX − WU), representing the primary exercise-induced response (Spearman's r = 0.89, 95% CI: 0.72–0.96, p << 0.017), thereby exceeding the Bonferroni-adjusted significance threshold (Fig. 4b). No statistically significant relationships were found for the remaining phases. For ΔWU, the Spearman correlation coefficient was r = 0.02 (p = 0.93), whereas for ΔCD it was r = 0.14 (p = 0.61).

4. Discussion

The present study aimed to examine the dynamics of normalized T_{sk} and muscle oxygen saturation across key exercise phases and to explore their potential physiological relationships. Although no statistically significant differences were observed between exercise phases after Bonferroni correction, several consistent tendencies emerged that warrant discussion.

Heat moves from the body's core to the skin mainly through the bloodstream. So, control of blood flow is a key part of this process, affecting both muscles and skin, specifically, involving the blood flow to skeletal muscles, referred to as muscle blood flow (MuBF), and the blood flow in the skin, known as skin blood flow (SkBF) [39]. During physical activity, the increased blood flow to the working muscles helps deliver oxygen, transport nutrients, and remove metabolic heat from the body. Simultaneously, the gradual widening of blood vessels in the skin facilitates heat transfer from the body's surface to the surrounding environment [22].

During physical exercise, elevated muscle metabolism and perfusion substantially increase the amount of heat transported by the circulatory system [18]. Despite its simplifying assumptions, such as neglecting blood flow directionality, the Pennes bioheat equation provides a useful theoretical framework for describing temperature distribution in biological tissues and for conceptualizing the role of blood perfusion in thermoregulation during exercise. In the present study, the model is used solely to support the physiological interpretation of the observed thermal responses, as none of its parameters were directly measured [pennes!]. In the context of endurance sports, the Pennes bioheat model serves as a conceptual framework for interpreting changes in Tsk and local muscle hemodynamics observed with increasing exercise intensity.

A critical aspect of NIRS data interpretation is the identification of breakpoints in muscle oxygenation profiles. Previous studies have demonstrated moderate to high agreement between SmO_2 breakpoints and ventilatory thresholds determined via gas exchange analysis during both

cycling and running [11]. Despite its numerous advantages, NIRS has certain limitations, including limited penetration depth and increased variability at high exercise intensities. Additionally, researchers have reported substantial inter-individual differences and potential inter-limb asymmetries that are not always related to limb dominance [34]. Therefore, NIRS is best suited for monitoring relative changes within the same muscle and individual over time.
In summary, NIRS represents a valuable method for assessing local muscular responses to physical exertion, offering insights into the regulation of oxygen delivery and utilization at the muscle level and complementing traditional physiological indicators such as heart rate, oxygen uptake, and blood lactate concentration [29].

The lack of statistically significant pairwise differences in T_{sk_rel} across phases may reflect the combined influence of relatively small sample size and inter-individual variability in thermoregulatory responses. Exercise-induced T_{sk} dynamics are governed by the interactions among metabolic heat production, local muscle perfusion, and heat-dissipation mechanisms. During dynamic cycling, an initial cutaneous vasoconstriction may occur despite increasing metabolic demand, followed by vasodilation as thermoregulatory processes become dominant [16],[20]-[22]. For changes in normalized T_{sk_rel} across exercise phases, no statistically significant pairwise differences were identified after Bonferroni correction, although the lowest p-value obtained was 0.012. Given the relatively small cohort (n = 8), the statistical power to detect subtle yet biologically meaningful differences was limited. Nevertheless, the observed pattern of responses suggests that structured thermal adjustments accompany incremental exercise (Fig. 2).
A similar pattern was observed for relative SmO_{2_rel}. Although differences between phases did not reach corrected significance levels, a clear trend toward modulation across exercise stages was evident (Fig. 3). Only a trend toward significance was observed (p = 0.012), potentially reflecting limited statistical power due to the relatively small sample size. Muscle oxygen saturation reflects the dynamic balance between oxygen delivery and extraction. During the warm-up phase, enhanced blood flow may temporarily increase oxygen availability, whereas an increased workload typically increases oxygen extraction and reduces SmO_2 [7],[25],[35],[37]. The directional changes observed across phases are therefore physiologically coherent and consistent with known microvascular and mitochondrial adjustments to incremental load. Inter-individual variability likely attenuated group-level contrasts, yet the overall trajectory of responses suggests meaningful oxygenation dynamics [35].

The most noteworthy finding was the strong positive correlation between ΔEX in normalized T_{sk} and ΔEX in normalized SmO_2 (Spearman's r = 0.89, 95% CI: 0.72–0.96, p < 0.001), as shown in Figure 4. This moderate relationship suggests that individuals who demonstrate greater exercise-induced changes in muscle oxygenation also exhibit larger changes in the T_{sk} overlying the rectus femoris. This supports the idea that perfusion-related adjustments simultaneously influence oxygen availability and convective heat transfer. It should be noted that, due to the small sample size (n = 8), the present correlations were analyzed at the observational level and should be interpreted as descriptive of physiological connections rather than indicative of causal relationships.

Physiologically, increased oxygen delivery during exercise is mediated by augmented blood flow, which concurrently enhances heat transport from active muscle to the skin surface. Individuals with more pronounced perfusion responses would therefore be expected to demonstrate parallel shifts in SmO_2 and T_{sk} [17],[20],[22],[36],[37]. Notably, this association was specific to the exercise phase, suggesting that the coupling between oxygenation and thermal signals is most evident when metabolic demand and circulatory adjustments are at their peak. During warm-up and recovery, preparatory or redistributive hemodynamic processes may partially uncouple these signals [15],[20]-[22].

The observed correlations between muscle oxygen saturation and T_{sk} can be interpreted within the theoretical framework of the Pennes bioheat model, which describes the relationship between metabolic heat production and blood perfusion. Although the physiological parameters of the model were not directly measured in the present study, the Pennes equation provides a conceptual basis for interpreting the coupling between muscle oxygenation and thermal responses during exercise. Within this framework, fluctuations in NIRS-derived oxygenation may reflect changes in local oxygen extraction and microvascular blood flow, which in turn may influence convective heat transfer and the Tsk distribution detected by IRT. Accordingly, the parallel modulation of thermal and oxygenation parameters observed during incremental exercise is consistent with the concept that both signals reflect complementary aspects of the underlying hemodynamic and metabolic responses [24],[28],[33].

Importantly, the coupling between ΔEX T_{sk_rel} and ΔEX SmO_{2_rel} aligns with findings reported by Vasquez-Bonilla et al., who also demonstrated coordinated changes in T_{sk} and muscle oxygenation during exercise [35].

Taken together, the identified trends and phase-specific relationships suggest that integrating thermal imaging with NIRS-derived muscle oxygenation provides complementary insight into

local muscular responses during dynamic exercise. Considering the good-to-excellent reliability of SmO_2 documented across exercise intensities (Yogev et al., 2023) [40], this multimodal approach seems promising for monitoring internal load and training adaptation and for potentially detecting functional asymmetries in athletic populations.

5. Conclusions

The present findings suggest that increasing exercise intensity may be accompanied by concurrent alterations in muscle oxygenation and Tsk distribution, reflecting complex hemodynamic and metabolic adjustments to physical load. The integrated protocol combining infrared thermography (IRT) and near-infrared spectroscopy (NIRS) produced coherent and physiologically plausible response patterns. This supports the methodological feasibility of the protocol when carried out under standardized incremental exercise conditions.

Importantly, due to its non-contact and rapid acquisition characteristics, IRT may represent a practical alternative in certain monitoring contexts. Unlike NIRS, which provides localized measurements limited to a specific sensor placement, IRT enables assessment of the entire skin surface overlying the active muscle, offering a spatially comprehensive view of thermal distribution. This broader perspective may enhance the detection of regional asymmetries and heterogeneous perfusion patterns, potentially increasing ecological validity in applied sports or clinical settings.

Although the observed relationships should be interpreted with caution due to the small sample size, the proposed measurement approach offers a valid framework for the multidimensional assessment of local muscular responses. This combined protocol could therefore serve as a basis for future studies involving larger groups of participants, aimed at confirming and further elucidating the relationship between thermal and oxygenation dynamics during exercise.

At the same time, both NIRS and IRT require careful interpretation, taking into account technical constraints and individual factors, such as adipose tissue thickness and environmental conditions.

Future studies involving larger cohorts are warranted to confirm the present findings and to enable more advanced analyses, including breakpoint analysis and modeling of SmO_2 responses as a function of exercise intensity.

Acknowledgments

The authors would like to thank all participants for their time and commitment to this research.

Funding

The research activities were co-financed by the funds granted under the Research Excellence Initiative of the University of Silesia in Katowice.

Conflict of interest

The authors declare that they have no conflict of interest.

References

1. Ammer K., The Glamorgan Protocol for recording and evaluation of thermal images of the human body, Thermol Int, 2008, 18(4):125–144.
2. Ashworth E.T. Sweat evaporation in humans: A molecular and thermodynamic perspective, Exp Physiol, 2026, 111(3):643-652, DOI: 10.1113/EP093011.
3. Barton M., Larson D., Lantis D., Farrell J., Cantrell G., Shipman S., Larson R., Comparison between VO2max cycling protocols, American College of Sports Medicine Annual Meeting, 2014, DOI: 10.13140/RG.2.1.1489.9682.
4. Bassett D.R., Howley E.T., Limiting factors for maximum oxygen uptake and determinants of endurance performance, Med Sci Sports Exerc, 2000, 32(1):70–84.
5. Bompa T.O., Buzzichelli C.A., Periodization – Theory and Methodology of Training, Human Kinetics, Champaign, 2019.
6. Brooks G.A., The lactate shuttle during exercise and recovery, Med Sci Sports Exerc, 1986, 18(3):360–368, DOI: 10.1249/00005768-198606000-00019.
7. Calbet J.A., Boushel R., Radegran G., Sondergaard H., Wagner P.D., Saltin B., Determinants of maximal oxygen uptake in severe acute hypoxia, Am J Physiol Regul Integr Comp Physiol, 2003, 284:R291–R303, DOI: 10.1152/ajpregu.00155.2002. t
8. Crum E.M., O'Connor W.J., Van Loo L., Valckx M., Stannard S.R., Validity and reliability of the Moxy oxygen monitor during incremental cycling exercise, Eur J Sport Sci, 2017, 17(8):1037–1043, DOI: 10.1080/17461391.2017.1330899.
9. da Silva J.C., Tarassova O., Ekblom M.M., Andersson E., Rönquist G., Arndt A., Quadriceps and hamstring muscle activity during cycling as measured with intramuscular electromyography, Eur J Appl Physiol, 2016, 116(9):1807–1817, DOI: 10.1007/s00421-016-3428-5.
10. Faria E.W., Parker D.L., Faria I.E., The science of cycling: physiology and training – Part 1, Sports Med, 2005, 35(4):285–312.

11. Feldmann A., Ammann L., Gächter F., Zibung M., Erlacher D., Muscle oxygen saturation breakpoints reflect ventilatory thresholds in both cycling and running, J Hum Kinet, 2022, 83:87–97, DOI: 10.2478/hukin-2022-0054.
12. Feldmann A., Schmitz R., Erlacher D., Near-infrared spectroscopy-derived muscle oxygen saturation on a 0% to 100% scale: reliability and validity of the Moxy Monitor, J Biomed Opt, 2019, 24(11):115001, DOI: 10.1117/1.JBO.24.11.115001.
13. Friel J., The Mountain Biker's Training Bible, VeloPress, Colorado, 2000.
14. Górski J., Human Physiology (in Polish), Wydawnictwo Lekarskie PZWL, Warsaw, 2010.
15. Górski J., Physiology of Exercise and Physical Training (in Polish), PZWL, Warsaw, 2011.
16. Guyton A.C., Hall J.E., Textbook of Medical Physiology, 11th ed., Elsevier Inc., Philadelphia, 2006.
17. Herman I.P., Physics of the Human Body, Springer, New York, 2016.
18. Huang H.-W., Horng T.-L., Bioheat transfer and thermal heating for tumor treatment, [in:] Heat Transfer and Fluid Flow in Biological Processes, Academic Press, 2015, 1–42, DOI: 10.1016/B978-0-12-408077-5.00001-8.
19. Impellizzeri F.M., Marcora S.M., The physiology of mountain biking, Sports Med, 2007, 37(1):59–71.
20. Karlsson J., Jacobs I., Onset of blood lactate accumulation during muscular exercise as a theoretical concept, Int J Sports Med, 1982, 3:190–193.
21. Kellogg D.L., Johnson J.M., Kosiba W.A., Control of internal temperature threshold for active cutaneous vasodilation by dynamic exercise, J Appl Physiol, 1991, 71:2476–2482.
22. Kenney W.L., Johnson J.M., Control of skin blood flow during exercise, Med Sci Sports Exerc, 1992, 24:303–312.
23. MacDougall D., Sale D., The Physiology of Training for High Performance, Oxford University Press, Oxford, 2014.
24. Majchrzak E., Numerical modelling of bio-heat transfer using the boundary element method, J Theor Appl Mech, 1998, 36(2):437–455.
25. Miranda-Fuentes C., Chirosa-Rios L., Guisado-Requena I., García-Pinillos F., Del-Cuerpo I., López-Fuenzalida A., Ibacache-Saavedra P., Jerez-Mayorga D., Can strength exercise affect the muscle oxygen saturation response?, Acta Bioeng Biomech, 2022, 24(2):37–45, DOI: 10.37190/ABB-02021-2022-03.

26. Moreira D.G., Costello J.T., Brito C.J., et al., Thermographic imaging in sports and exercise medicine: a Delphi study and consensus statement on the measurement of human skin temperature, J Therm Biol, 2017, 69:155–162, DOI: 10.1016/j.jtherbio.2017.07.006.
27. Mujika I., Halson S., Burke L.M., Balague G., Farrow D., An integrated, multifactorial approach to periodization for optimal performance in individual and team sports, Int J Sports Physiol Perform, 2018, 13:538–561.
28. Pennes H.H., Analysis of tissue and arterial blood temperatures in the resting human forearm, J Appl Physiol, 1948, 1(2):93–122.
29. Perrey S., Quaresima V., Ferrari M., Muscle oximetry in sports science: an updated systematic review, Sports Med, 2024, 54(4):975–996, DOI: 10.1007/s40279-023-01987-x.
30. Pocock G., Richards C.D., Richards D.A., The respiratory system, [in:] Human Physiology, 5th ed., Oxford University Press, Oxford, 2018.
31. Possamai L.T., Campos F.S., Salvador P.C.D.N., et al., Similar maximal oxygen uptake assessment from a step cycling incremental test and verification tests on the same or different day, Appl Physiol Nutr Metab, 2020, 45(4):357–361, DOI: 10.1139/apnm-2019-0405.
32. Rowbottom D.G., Periodization of training, [in:] Garrett W.E., Kirkendall D.T., Exercise and Sport Science, Lippincott Williams & Wilkins, Philadelphia, 2000.
33. Shrivastava D., Vaughan J.T., A generic bioheat transfer thermal model for a perfused tissue, J Biomech Eng, 2009, 131(7):074506, DOI: 10.1115/1.3127260.
34. Skotzke P., Schwindling S., Meyer T., Side differences and reproducibility of the Moxy muscle oximeter during cycling in trained men, Eur J Appl Physiol, 2024, 124(10):3075–3083, DOI: 10.1007/s00421-024-05514-2.
35. Vasquez-Bonilla A.A., Boschetti F., Yañez Sepulveda R., Sillero-Quintana M., Effects of exercise intensity on skin temperature and muscle oxygen saturation in the thigh during and after strength resistance training, J Therm Biol, 2025, 130:104132, DOI: 10.1016/j.jtherbio.2025.104132.
36. Villar R., Hughson R.L., Vascular conductance and muscle blood flow during exercise are altered by inspired oxygen fraction and arterial perfusion pressure, Physiol Rep, 2017, 5(5):e13144, DOI: 10.14814/phy2.13144.
37. Walker K.L., Saunders N.R., Jensen D., Kuk J.L., Wong S.L., Pyke K.E., Do vasoregulatory mechanisms in exercising human muscle compensate for changes in

arterial perfusion pressure?, Am J Physiol Heart Circ Physiol, 2007, 293:H2928–H2936.

38. Wasserman K., Whipp B.J., Koyl S.N., Beaver W.L., Anaerobic threshold and respiratory gas exchange during exercise, J Appl Physiol, 1973, 35(2):236–243.
39. Wendt D., van Loon L., van Marken Lichtenbelt W., Thermoregulation during exercise in the heat, Sports Med, 2007, 37(8):669–682.
40. Yogev A., Arnold J., Nelson H., Clarke D.C., Guenette J.A., Sporer B.C., Koehle M.S., Comparing the reliability of muscle oxygen saturation with common performance and physiological markers across cycling exercise intensity, Front Sports Act Living, 2023, 5:1143393, DOI: 10.3389/fspor.2023.1143393.